Biophysical Chemistry, 38 (1990) 11–22
Elsevier

BIOCHE 01454

Environment-induced changes in DNA conformation as probed by ethidium bromide fluorescence

Carla Cuniberti and Marina Guenza

Istituto di Chimica Industriale, Università di Genova, e Centro Studi Chimico Fisici di Macromolecole Sintetiche e Naturali, C.N.R., Corso Europa 30, 16132 Genova, Italy

Received 20 November 1989
Accepted 21 February 1990

DNA conformation; Ethidium intercalation; Ethidium fluorescence

The interaction of the ethidium cation with calf thymus DNA is investigated in solutions of different ionic strength and temperature by observation of the enhancement of fluorescence of ethidium upon intercalation in the duplex structure. The quantum yield of the fluorescence of the intercalated dye is found to increase either upon lowering the Na^+ concentration or upon increasing the temperature. The existence of a correlation between the geometry of the intercalation complex and the features of the secondary structure of DNA is suggested. Binding isotherms under corresponding environmental conditions are also quantitated by fluorescence enhancement and interpreted in terms of the neighbor exclusion model. Large contributions from change in hydration to the thermodynamics of binding are demonstrated by the temperature dependences of the equilibrium constants. The neighbor exclusion range is found to be practically independent of the salt concentration but its value increases from an average of 2.4 around room temperature to 4–5 at 80 °C, as inferred from the binding curves in 0.15 and 0.5 M $[Na^+]$ or from the DNA hypochromism vs temperature profiles of complexes at 10^{-3} M $[Na^+]$. All the data point to a possible sequence-conformation specificity in the intercalation of ethidium which in heterogeneous DNA is mediated by environmental changes.

1. Introduction

Current experimental and theoretical information about the conformational and dynamic properties of DNA points towards a double helical structure characterized by a much higher flexibility than was initially thought. Variations in gross structural parameters, such as the duplex winding angle θ and the distance between base planes h, have been observed for the B-DNA form both in the crystalline state and solution [1–3]. Molecular mechanics calculation [4–6] confirm that the B-geometry can undergo correlated variations in the dihedral rotation angles of the phosphate-sugar backbones and in the base-pairs' relative positions at relatively low energetic costs and without taking the DNA molecule out of the B-genus. Thus, thermal fluctuations drive the chain through continuous twisting and bending motions around its equilibrium structure, and changes in environmental conditions can easily trigger small permanent conformational distortions.

In dilute solutions, small but systematic variations of θ with temperature, electrolyte concentration and nature of the counterion have been assessed in a variety of studies [3,7–10]. In general, the duplex unwinds with respect to the standard B-DNA either by increasing the temperature or decreasing the salt concentration. If the coupling of unwinding with the increment of the distance between base is considered [11], from the experimental observations discussed above one may in-

Correspondence address: C. Cuniberti, Istituto di Chimica Industriale, Università di Genova, 16132 Genova, Italy.

fer that the mean step height will be somewhat higher than the standard value of 3.4 Å of B-DNA, either at low ionic strength or in the premelting region. The suggestion made by Chan et al. [9], that the temperature has a discriminatory effect on the relative contribution of the GC and AT base-pairs to the variation of the duplex winding angle, as detected in the circular dichroism spectra, is in line with the differences in the premelting effects found for synthetic duplexes with defined sequences [12]. Accordingly, the fine structure of deoxyoligonucleotides in the crystalline state has been observed to depend on the sequence of base-pairs [2].

It is believed that the structural flexibility of the DNA helix, time scale of conformational fluctuations and local variations of helical parameters due to specific base sequences are important because of their potential roles in the mechanisms of DNA replication, transcription and drug binding. Therefore, we have considered it of interest to study how the subtle changes induced by temperature and salt concentration may affect the mode of binding of an intercalative drug.

The ethidium cation, or 3,8-diamino-5-ethyl-6-phenylphenantridinium, is a well-known intercalative agent of nucleic acids with double helical structure [13]. The large fluorescence enhancement it displays upon formation of the intercalation complex [14] has determined its extensive utilization as a fluorescent probe of the topological [15–19] and dynamical [20–27] properties of DNA, also because the binding affinity and the fluorescence enhancement are practically independent of the base composition [13,28,29]. The intercalation models proposed for the ethidium-DNA complex [30,31] envisage the planar phenantridinium ring as being inserted between base-pair planes in such a way that the two 3.8-amino substituents can establish hydrogen bonds with the phosphate groups across the two DNA strands. These hydrogen bonds appear to play the role of maintaining the ethidium cation in a specific orientation with respect to the polymer frame. Indeed, phenantridinium derivatives lacking the 3-amino group or both the 3,8-substituents form much weaker complexes than ethidium and at the same time show lower or absent fluorescence enhancement [32]. From these results, a connection between the hydrogen bonding to the two helix strands with the complete insertion of the drug within the hydrophobic pocket of the base-pair system and with the consequent increase of the fluorescence emission is evident.

In this work we have carried out measurements designed to elucidate the influence of the double helix conformation on the positioning of the ethidium cation within the DNA intercalation site based on the hypothesis of a correlation between the fluorescence quantum yield of the intercalated dye and the geometry of the complex. The variation of the fluorescence quantum yield of the dye intercalated into native DNA from calf thymus in aqueous solutions at different ionic strengths and temperatures has been studied. Increasing the temperature or lowering the ionic strength appeared to produce similar increases of the quantum yield. Thus, it seems that a more unwound duplex conformation allows a better realization of those interactions which are responsible for the fluorescence enhancement. Full analysis of the binding equilibria from fluorometric titration curves has shown that the DNA conformational features also affect somewhat the size of the binding site. The increase in size of the binding site with temperature has also been demonstrated at low ionic strength from the analysis of the spectrophotometric melting behavior of DNA in complexes of increasing degree of saturation.

2. Experimental

2.1. Materials

Calf thymus deoxyribonucleic acid (CT-DNA) was purchased from Sigma (sodium salt, highly polymerized sample). Stock solutions were routinely prepared in 1 mM Tris, pH 7.5 buffer solution [33]. The final stock solution was frozen and stored at $-20\,^{\circ}C$. When needed, weighed amounts of the stock solution were appropriately diluted and the concentration measured spectrophotometrically, using a molar absorption coefficient of $\epsilon = 13200\ M^{-1}\ cm^{-1}$ at 260 nm. From the absorbance ratio $A(280)/A(260) < 0.54$, a re-

sidual protein content lower than 1% was estimated and the hyperchromic effect from spectrophotometric melting curves was found to agree with reported data for CT-DNA [34]. The ionic strength of dilute CT-DNA solutions in 1 mM Tris was evaluated as 1.05×10^{-3} ($\pm 0.15 \times 10^{-3}$) from the observed value of the CT-DNA transition temperature ($T_m = 46 \pm 1°C$) and using the ionic strength dependence of T_m reported in the literature [35].

Ethidium bromide (EB) was also obtained from Sigma. The dye, tested by thin-layer chromatography, ^{1}H-NMR and thermogravimetric analysis, was found to be free from coloured impurities and to contain 0.12 mol of ethanol plus 0.64 mol of water per mol of EB [36]. Stock solutions of the dye in buffer were prepared by weight and stored at 4°C in foil-wrapped bottles. Under these conditions, the stock solutions were spectrophotometrically stable for several weeks. A molar absorption coefficient of 5850 $M^{-1}\,cm^{-1}$ at 480 nm was used to determine the concentration of dilute aqueous EB solutions at 20°C, independently of the ionic strength [36].

Salts and other chemicals were of Merck, suprapur grade quality. Deionized water was distilled before use.

2.2. Methods

Absorption spectra were recorded on a Varian Cary 219 spectrophotometer equipped with the cell temperature reading accessory. The visible band of EB in dilute solution was recorded at increasing DNA/EB ratio in order to determine the position of the isosbestic point which is known to characterize the binding equilibrium [28] and to evaluate the spectrum of bound dye under different environmental conditions.

Fluorescence spectra were obtained by means of a Perkin Elmer MPF-44A spectrofluorimeter equipped with a DSCU-2 spectral correction unit, operated in the ratio mode. Monitoring of the temperature was accomplished with a thermocouple inserted in the reference cell and connected with a digital readout display. Dye excitation, either in solutions of free EB or in the presence of CT-DNA, was performed at the isosbestic point previously determined spectrophotometrically. The fluorimeter performance was routinely checked with a dilute rhodamine B solution in polymethylmethacrylate glass.

Jacketed cell holders connected to liquid circulating thermostatic baths maintained a constant temperature with an accuracy of $\pm 0.1°C$ in both spectrophotometric and spectrofluorimetric experiments.

The spectrophotometric thermal transition of CT-DNA was studied at low ionic strength at different EB/DNA ratios. The corresponding dependence of EB fluorescence on temperature was monitored at 595 nm. These experiments were carried out at a constant heating rate of 1 degree/min with the aid of electronic temperature programmers connected to the circulating baths.

All experiments were performed in 1 mM Tris buffer, pH 7.5, with no added salt or at 0.15, 0.5, 1 M NaCl, respectively. In order to consider the EB dimerization negligible [36], the dye concentration was always kept below $2–3 \times 10^{-5}$ M. All solutions were prepared gravimetrically.

The absorption and emission data were transferred to an IBM-XT2 graphic desk computer as one data point at 1-nm intervals for the spectra or as one data point per degree in the variable temperature experiments at constant wavelength and stored for further analysis. Standard programs in BASIC language for linear or nonlinear least-squares fitting to experimental data were used in some cases. An iterative nonlinear least-squares program based on Newton's method [36,37] was applied to evaluate the binding parameters from the experimental binding isotherms.

2.3. Absorption and fluorescence data analysis

According to the usual procedure in employed spectrophotometric studies of EB binding to DNA, the absorbance A at each wavelength within the visible absorption band of a solution at a given EB/DNA ratio was considered additive with respect to the contributions of the free and bound dye species. The fraction, X_b, of dye bound to DNA was calculated from the relative absorbance A/A^0 according to:

$$X_b = \left[(A/A^0) - 1\right] / \left[(\epsilon_b/\epsilon_f) - 1\right] \quad (1)$$

where A^0 refers to the EB solution in the absence of DNA and ϵ_b/ϵ_f denotes the bound-to-free EB absorption coefficient ratio. The evaluation of ϵ_b/ϵ_f was made at DNA/EB $\gg 1$, where the binding equilibrium gives:

$$A^0/(A - A^0) = [1/R_a - 1][1 + 1/KP] \qquad (2a)$$

or, alternatively:

$$PA^0/(A - A^0) = [1/R_a - 1][(1/K) + P] \qquad (2b)$$

where $R_a = \epsilon_b/\epsilon_f$, K is the apparent association constant and P the CT-DNA concentration (in mol base-pairs per l).

We used both eqs 2a and 2b to obtain R_a from the intercept of $A^0/(A - A^0)$ vs $1/P$ and from the slope of $PA^0/(A - A^0)$ vs P, respectively, and considered the average of these two values as the final result. Then, from R_a and ϵ_f as a function of wavelength, the absorption spectrum of EB intercalated into CT-DNA under different environmental conditions was evaluated. In 0 M NaCl solutions, the spectrum of bound EB was directly observed at DNA/EB > 5, owing to the very large value of the binding constant K at low ionic strength [14,28].

Since a blue shift and narrowing of the fluorescence band are observed upon binding of EB to DNA as compared to the emission spectrum of the free dye, it is not correct to consider the fluorescence intensity at a fixed wavelength as linear in the quantum yield contributions from the free and bound species in equilibrium. In order to evaluate the total emission, the observed fluorescence spectrum was in each case corrected for the wavelength dependence of the receiving system in the range from 540 to 700 nm. Correction factors were derived either by means of the DSCU-2 unit or by comparing recorded spectra of standard fluorophores to the correct ones. Since this procedure did not provide the complete correct emission spectra, the area of the emission band was approximated by the product of the maximum intensity, I_{max}, times the correspondent bandwidth.

The emission area F from the spectrum of an EB/DNA solution relative to the area F^0 of the corresponding solution of free EB can thus be considered as equal to the quantum yield ratio ϕ/ϕ^0 at any EB concentration if the excitation wavelength is chosen to be coincident with the isosbestic point. Of course, this procedure requires the use of solutions with negligible fluorescence reabsorption. In this case, a relationship between ϕ/ϕ^0 and X_b equivalent to eq. 1 can be written:

$$X_b = [(\phi/\phi^0) - 1]/[(\phi_b/\phi_f - 1)] \qquad (3)$$

where now ϕ_b/ϕ_f (henceforth denoted R_e) is the bound-to-free fluorescence quantum yield ratio of monomeric EB.

The R_e values were then obtained by applying the procedures corresponding to eqs 2 and 2b to the data $\phi^0/(\phi - \phi^0)$ from the titrations of EB with increasing concentrations of CT-DNA. The environmental dependence of the quantum yield, ϕ_f, of free EB, was checked by measuring the fluorescence emission of low absorbance solutions at fixed excitation wavelength (either 480 or 510 nm) and after correcting for the absorbance and refractive index changes. The reference value $\phi_f = 0.019$ was considered in 0.15 M NaCl at 20 °C [38]. From the coupled data R_e and ϕ_f, the quantum yield ϕ_b of EB intercalated into the CT-DNA duplex was then derived.

2.4. Binding isotherms

The number of bound ethidium cations per base-pair, r, was determined from ϕ/ϕ^0 obtained by titrating fixed amounts of CT-DNA with EB and using eq. 3 with the appropriate value of R_e. From these data the conventional Scatchard plots, r/C_f vs r, were constructed in order to determine the binding parameters.

It has been shown [39,40] that in intercalative drug binding to DNA, there is a site-exclusion effect that causes nonlinearity of the Scatchard plot through an assocation constant $K(r)$ which is a function of r. This modified Scatchard expression is given by:

$$\frac{r}{C_f} = K(1 - nr)\left[\frac{1 - nr}{1 - (n-1)r}\right]^{n-1} \qquad (4)$$

where K is the site association constant at $r \to 0$ and n represents the number of sites excluded per bound ligand.

In the classic intercalation model the exclusion number n is equal to two, i.e., the two free sites which are nearest neighbors to the intercalated base-pair are excluded from binding. However, we let both K and n as unknown parameters be determined by fitting eq. 4 to the experimental data.

2.5. Temperature profiles of CT-DNA absorbance and EB fluorescence

Temperature-absorbance profiles of CT-DNA at 260 nm were recorded in 1 mM Tris, pH 7.5, solutions at increasing EB/DNA ratio. After correcting for the volumetric expansion with temperature, the curves were transformed to hyperchromicity h vs temperature. Derivative curves were calculated as $[h(T+\Delta T)-h(T)]/\Delta T$ vs the mean temperature $\Delta T/2+T$, with $\Delta T=1°$. The areas of the derivative curve were then calculated by computer integration.

Corresponding temperature-fluorescence profiles were recorded at 595 nm, the wavelength of maximum uncorrected emission from intercalated EB, with excitation fixed at 510 nm. After correcting the observed intensity for the decrease in concentration and in refractive index with increasing temperature, the ratio $[I(T)/I(20)]$ vs T was obtained.

3. Results

3.1. Optical properties of free and CT-DNA bound ethidium

Results previously obtained studying the EB dimerization in aqueous salt solution at 20 °C have shown that both the position of the absorption maximum and the molar absorption coefficient of the visible band of free monomeric EB do not depend on the NaCl concentration, at least up to 1 mol/l [36]. In contrast, in the present work, a significant temperature effect on this band was observed. The bathochromic and slightly hyperchromic shift on increasing the temperature was found to be reproducible in solutions containing 0, 0.15, 0.5 and 1 mol/l of NaCl, respectively.

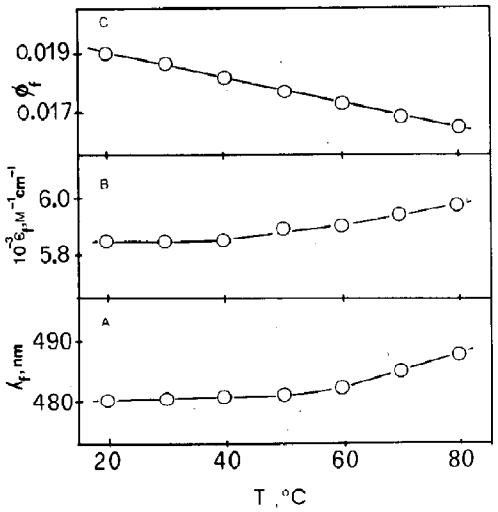

Fig. 1. Temperature dependence of the photophysical properties of free EB in aqueous solutions: (A) wavelength and (B) molar absorption coefficient at the maximum of the visible band; (C) fluorescence quantum yield.

Correspondingly, no apparent change in the fluorescence spectrum of free EB was caused by changing either the ionic strength or the temperature but the expected decrease in the emission intensity on increasing the temperature. Fig. 1 summarizes the temperature effects observed in the visible absorption band and fluorescence quantum yield of free EB in NaCl solutions in the range from 20 to 80 °C.

Relative to the visible absorption of the free monomer at room temperature, the absorption maximum of DNA-bound EB is red-shifted by 1600 cm^{-1} and is about 30% hypochromic. Similarly to free EB, the visible absorption band of the intercalated ethidium cation was found to be independent of the NaCl concentration. However, unlike free EB, the temperature dependence was found to be practically absent. From the experimental point of view, the different temperature effects on the free and bound species give rise to a red shift of the isosbestic point of the equilibrium mixture on increasing the temperature. In order to maintain constant the EB absorbance at the excitation wavelength in the fluorescence experiments, independently of the relative amount of bound/free dye at each temperature, λ_{exc} had to be

Table 1

Bound-to-free quantum yield ratio of ethidium in complexes with CT-DNA at different NaCl concentrations and temperatures

The average standard deviation amounts to ±4%.

T (°C)	R_e			
	0	0.15	0.5	1
20	10.4	10.3	9.6	9.2
25	10.75	10.7	9.7	–
30	11.2	10.9	9.9	–
35	11.2	11.2	10.15	9.4
38	11.4	–	–	–
45	12.0	12.2	10.7	–
70	–	13.4	12.5	10.7
80	–	14.5	13.3	11.2

shifted according to the shift in the isosbestic point.

Also, the fluorescence spectrum of the DNA-bound ethidium showed no apparent change in position and shape on varying the salt concentration or the temperature. However, a small but meaningful dependence of the quantum yield on environmental conditions was detected. In table 1, the quantum yield ratio R_e measured at different NaCl concentrations and temperatures is reported. From these data, after multiplying by the corresponding value of ϕ_f (fig. 1), the quantum yield of intercalated ethidium, ϕ_b, vs temperature shown in fig. 2 for the different salt solutions was obtained. It is evident that the usual thermal quenching effect, indeed observed in free EB, is here totally absent. Instead, ϕ_b exhibits a systematic increase on increasing the temperature in all the solutions examined. Thus, the intercalated molecule appears to be more sensitive to the changes in its interactions with the duplex frame than to thermally activated quenching processes. Also, the smaller values of ϕ_b found at higher ionic strength are not related to the behavior of free ethidium (neither Na^+ nor Cl^- acts as a direct quencher of the dye fluorescence), again suggestive of the presence of a correlation between the secondary structure of the DNA duplex and the fluorescence emission of bound ethidium.

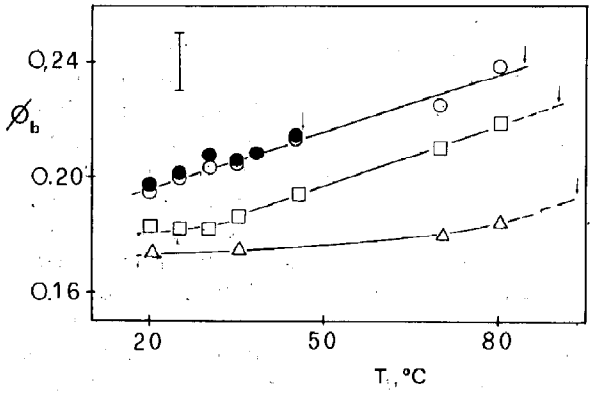

Fig. 2. Temperature dependence of the fluorescence quantum yield of EB intercalated in DNA at different ionic strengths: $[Na^+] = 10^{-3}$ (●), 0.15 (○), 0.5 (□), 1 (△) mol/l. The error bar represents the maximum deviation observed in ϕ_b. The arrows indicate the melting temperatures of free CT-DNA.

3.2. Binding parameters

Figs 3–6 present the Scatchard plots derived from the fluorimetric experiments for ethidium binding to CT-DNA under different solution conditions. The full curves through the data points represent the results of the fit by the neighbor

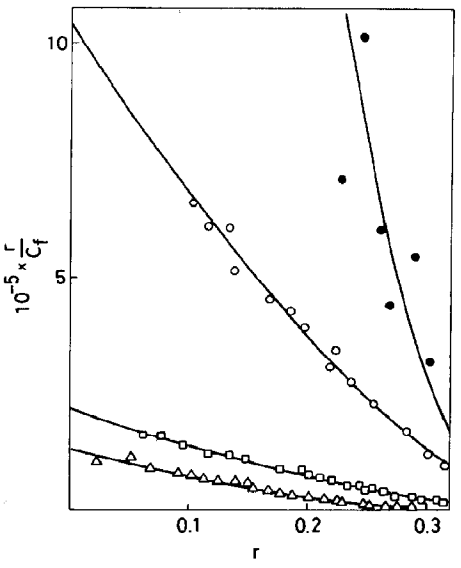

Fig. 3. Experimental and calculated neighbor exclusion binding isotherms for EB-CT DNA at 20 °C in 10^{-3} (●), 0.15 (○), 0.5 (□) and 1 (△) M $[Na^+]$. Values of K and n are given in table 2.

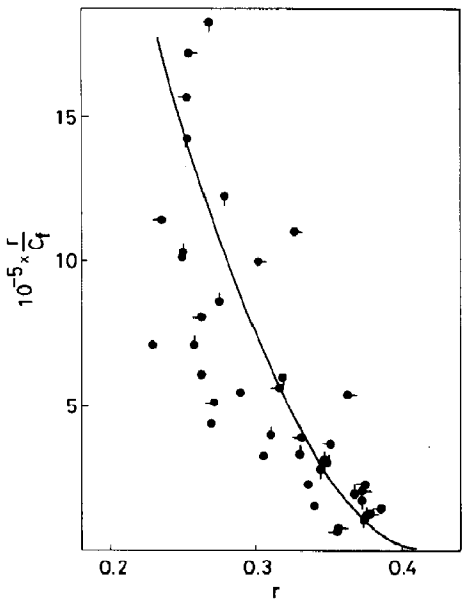

Fig. 4. Experimental and calculated neighbor exclusion binding isotherms for EB-CT DNA in 10^{-3} M [Na^+] at 20 (●), 25 (●), 35 (●), 38 (●) and 45 (●) °C. Values of K and n are given in table 2.

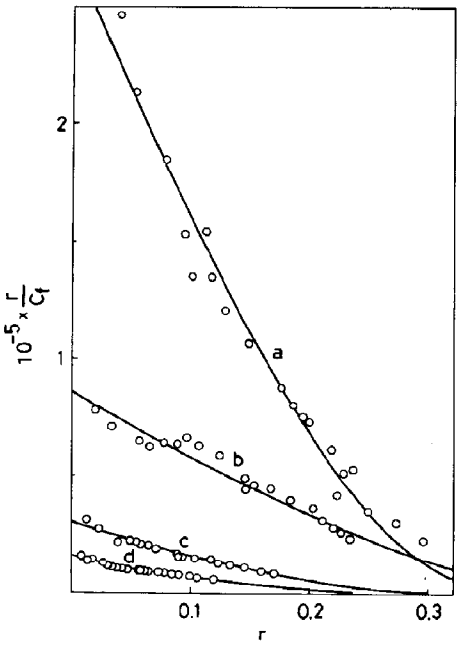

Fig. 5. Experimental and calculated neighbor exclusion binding isotherms for EB-CT DNA in 0.15 M [Na^+] at 25 (a), 45 (b), 70 (c) and 80 (d) °C. Values of K and n are given in table 2.

exclusion model with the values of the binding parameters K and n listed in table 2.

It is evident that the extent of the neighbor exclusion range is practically temperature and salt independent from 20 to 45 °C, although the average value of n appears somewhat larger than the classic $n = 2$ which corresponds to the simple exclusion of the two binding sites near to the intercalated one. A noninteger n larger than 2 suggests that anticooperative interactions contribute to some extent to the binding mechanism. At 70–80 °C in 0.15–0.5 M NaCl the neighbor exclusion range is increased to 3–4. This increase falls in a region where the largest change of the quantum yield of fluorescence of the intercalated ethidium was also observed. Our suggestion is that both these effects derive from the formation of intercalation complexes having different geometries. This observation is consistent with a neighbor exclusion range of 3 observed for ethidium binding to double helices of the A family [40].

The binding constant K at fixed temperature decreases over the range of NaCl concentration

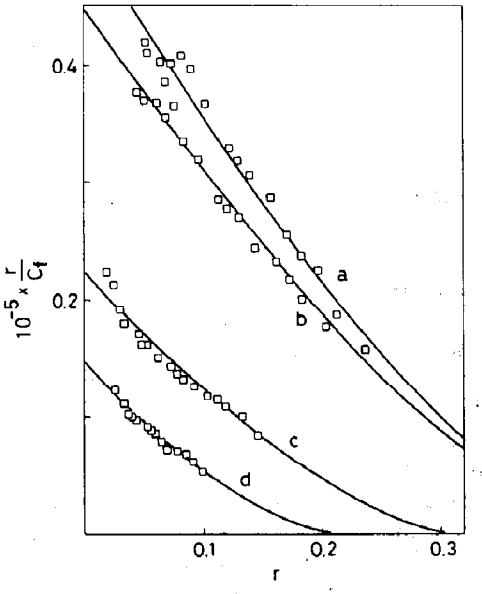

Fig. 6. Experimental and calculated neighbor exclusion binding isotherms for EB-CT DNA in 0.5 M [Na^+] at 30 (a), 35 (b), 70 (c) and 80 (d) °C. Values of K and n are given in table 2.

Table 2

Binding isotherms parameters for ethidium intercalation in CT-DNA at different NaCl concentration and temperature as obtained by the neighbor exclusion analysis

The average standard deviation amounts to ±10% in K and to ±7% in n.

T (°C)	[NaCl] (M)							
	0		0.15		0.5		1	
	n	10^{-5} K	n	10^{-5} K	n	10^{-5} K	n	10^{-5} K
20	2.7	64.0	2.3	10.4	2.4	2.13	2.7	1.25
25	2.3	41.6	2.7	2.71	–	–	–	–
30	–	–	2.6	2.54	2.1	0.51	–	–
35	2.2	42.1	2.6	2.22	2.1	0.45	–	–
38	2.2	76.2	–	–	–	–	–	–
45	2.4	89.6	2.2	0.86	–	–	–	–
70	–	–	3.1	0.30	2.9	0.22	–	–
80	–	–	3.5	0.15	4.1	0.14	–	–

from 0 to 1 M, as typically found for drug intercalation to DNA. The extent of the effect is well described by the electrostatic contribution to the overall interaction energy in the range of ionic strength from 0.1 to 1 [41]. The value at 1 mM Na^+ is, however, about two orders of magnitude lower than expected from the high ionic strength behavior. Since the uncertainty in the determination of such a large binding constant is very high, we have thoroughly analyzed the results from several sets of measurements. The average value of K at 1 mM Na^+, although affected by a large error (about 40%), could not reasonably become as high as the extrapolated datum. Instead, what cannot be completely excluded is that the observed decrease of ϕ/ϕ^0, exploited to calculate X_b, did in reality derive from the quenching of the fluorescence of intercalated ethidium that accompanies the onset of a secondary weak type of binding at low ionic strength and high EB/DNA ratio [14]. Since it is currently believed that the secondary binding takes place after saturation of the primary sites, we have taken care to stop our data collection at $r < 0.4$. Additionally, it should be noted that the titration curves at 1 mM Na^+ in the temperature range from 20 to 45 °C appear to be superimposed over each other, which is hardly compatible with the presence of two different binding mechanisms at binding ratios lower than 0.4. Thus, if the fluorescence data are considered to express the intercalation equilibrium, one may suggest that the more rigid highly hydrated helix conformation at low ionic strength [10] shows an affinity for ethidium intercalation smaller than the standard B-form would have under the same conditions. The resulting van't Hoff enthalpy equal to zero can be considered as evidence of an intercalation process which involves large contributions from the melting of hydration layers ($\Delta H > 0$) and release of melted water ($\Delta S > 0$) to the bulk medium.

The van't Hoff plots relative to the temperature dependence of the binding constants in 0.15 and 0.5 M NaCl solutions are given in fig. 7. The curves through the points represent the unweighed least-squares fits of the K data to the equation:

$$\ln K = A + B\left(1 - \frac{\theta}{T}\right) - C\left(\ln\frac{\theta}{T} + 1 - \frac{\theta}{T}\right) \qquad (5)$$

where θ represents a reference temperature and $A = -\Delta G^0(\theta)/R\theta$, $B = \Delta H^0(\theta)/R\theta$, $C = \Delta C_p^0(\theta)/R$, respectively [42]. Table 3 gives the values of the thermodynamic parameters derived from the fitting procedure for $\theta = 298$ K. The results from the measurements at low ionic strength are also included for comparison. The introduction of the temperature dependence of the enthalpy and entropy was found to be necessary

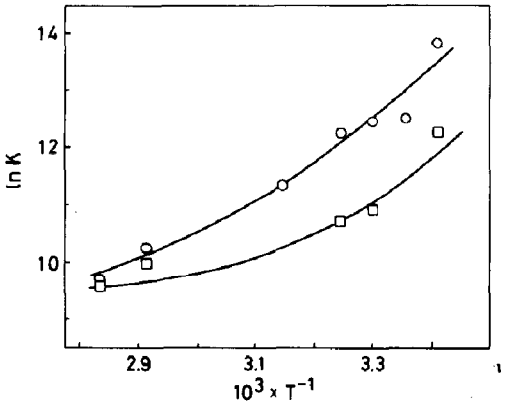

Fig. 7. Experimental and calculated van't Hoff plots for EB-CT DNA intercalation in 0.15 (○) and 0.5 (□) M [Na^+]. Values of the thermodynamic parameters are given in table 3.

Table 3

Thermodynamics of ethidium intercalation in CT-DNA at different ionic strength

$[Na^+]$ (M)	ΔG^0 (kcal mol^{-1})	ΔH^0 (kcal mol^{-1})	ΔS^0 (cal K^{-1} mol^{-1})	$\Delta C_p^{0\,a}$ (cal K^{-1} mol^{-1})
0.001	−8.99 [c]	0	30.2	–
0.15	−7.43	−16.1	−29.2	166
0.50	−6.58	−14.5	−26.6	295

[a] From the average value of K in the range 20–45 °C.

to account for the nonlinear behavior of ln K at high temperature. It is evident that at room temperature and high ionic strength the formation of the complex is driven by the binding enthalpy, as one might expect for an intercalating molecule. Our enthalpic and entropic terms are greater than the literature values for ethidium-DNA complexes under corresponding conditions [14,43], but the positive heat capacity term makes the two quantities less and less negative on increasing the temperature. One can infer from this that the release of water molecules contributes substantially to the intercalation process also at high ionic strength.

3.3. DNA melting and fluorescence profiles of complexes at low ionic strength

Fig. 8 shows typical differential melting curves of CT-DNA in 1 mM Tris buffer at several EB-to-base-pair ratios calculated from the hyperchromism measurements at 260 nm. The most evident feature in this figure is the biphasic nature of the melting of the duplex when $0 < r < 0.2$. The two melting phases correspond respectively to high melting ligand-saturated and low melting ligand-free lengths of the duplex [44]. By plotting the fraction of DNA melting at high temperature vs the degree of binding r one can calculate the size of the binding site [45]. Fig. 9 shows this type of plot derived from the melting curves. As units on the abscissa axis the ethidium-to-DNA input ratio (D/P) was used because at the ionic strength of these experiments it is practically equal to r. The fractional areas A_{II}/A_{TOT} were obtained by integration of the peaks after deconvolution of the curves of fig. 8 performed by assuming the shape

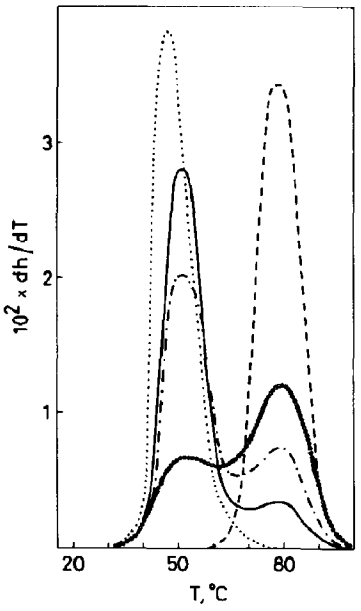

Fig. 8. Derivative profiles of CT-DNA hyperchromism vs temperature for EB/DNA = 0 (·····), 0.0167 (———), 0.0667 (·–·–·), 0.133 (○○○○○○), 0.200 (- - - - -) mol/b.p.m.; $[Na^+] = 10^{-3}$ M.

of the high melting component to be constant. From the slope of the linear plot through the data points a neighbor exclusion range $n = 5$ was derived. This finding confirms that the high temperature complex is characterized by a large exclusion range independently of the Na^+ concentration. A further significant feature to note is that the melt-

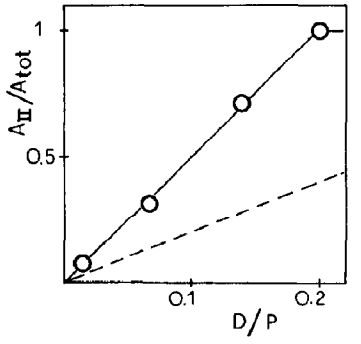

Fig. 9. Fraction of CT-DNA melting at high temperature (from curves of fig. 8) against the input ratio of dye molecules per base-pair.

ing temperature of the stabilized phase is only slightly, if at all, dependent on the overall value of D/P. This fact suggests that long ethidium-saturated regions tend to form on translocation of the drug from the random low temperature binding sites that melt to the rest of the still helical DNA. Also the very small shift of the low-melting peak relative to the melting point of the free duplex confirms that ethidium-free and ethidium-bound regions tend to segregate from each other.

From the relative change of the ethidium fluorescence measured at 595 nm as a function of temperature, $I(T)/I(20)$, apparently EB starts to be released from DNA around 55–60 °C and is totally released at around 95 °C where the fluorescence ratio becomes equal to that of the free dye. The range of temperature in which the dissociation takes place corresponds to that of the high melting peak in fig. 8 but the fluorescence curves are somewhat shifted to higher temperatures relative to DNA hypochromism. It is further observed that about 95 °C the fluorescence of ethidium does not acquire the temperature dependence characteristic of the free dye, but becomes completely quenched. This fact suggests that some kind of interaction between the ethidium cation and the polyanionic single-stranded chains takes place.

4. Discussion

The variation of the fluorescence quantum yield of ethidium bromide intercalated into heterogeneous natural DNA from calf thymus observed upon changing the salt concentration and temperature of the solution reveals that the detailed features of the EB-DNA complex depend on the overall structural properties of the binding sites on the duplex chain. The formation of the specific intercalation complex that corresponds to the models proposed [30,31] can take place if the DNA helix provides optimum dimensions not only for the full insertion of the phenantridinium ring but also for the building of the bridge across the duplex structure by hydrogen bonding the 3,8-amino substituents of ethidium with the phosphate groups of the polynucleotide strands. It is thus likely that the modification of the geometry of the binding sites may alter the orientation of the dye in such a way that, for instance, the amino groups of the dye can no longer bind to the phosphate groups of DNA but at the same time the phenantridinium ring is inserted into the helix. That the capacity of the dye to interact with nucleic acids depends on the specific structure of the polynucleotide chain more than on the chemical nature of the base sequence has been suggested on the basis of results of studies on the interactions of ethidium with double-helical synthetic polynucleotides [27,40].

The possibility that the observed variations of the fluorescence properties of the DNA-bound ethidium derive from the relative change of population of binding sites that might give rise to different fluorescence enhancements cannot be completely excluded at present. For instance, some variability in the binding constant to particular intercalation sequences present in natural DNAs is possible, however, it must be very small if practically no dependence of the binding parameters and/or of the fluorescence enhancement on the overall base composition has been found in previous studies [14,28].

On the other hand, a higher quantum yield has been measured in the present work on the ethidium complexes under conditions of salt concentration or temperature where the unwinding of the duplex structure relatively to the standard B-form has been found to take place [3,7–9]. The unwinding at low ionic strength can be understood as a general polyelectrolyte effect [11]. The extensive hydration of the helix under these conditions [46] may also contribute to the stabilization of the unwound state. It can be suggested that the better the insertion of the dye cation in the duplex the larger are the reduction of the electrostatic free energy and loss of hydration. At high ionic strength, it is more difficult for the ethidium cations to approach the binding sites because of the shielding effect from Na^+. At the same time, residual hydration layers are more tightly bound and a larger local unwinding angle would be required to transform the more wound helix to the exact geometry of the low ionic strength complex. Indeed, to explain the spectral changes in linear

and circular dichroism measurements shown by several dye-DNA complexes with salt concentration, it has been proposed [47] that the main effect of salt is to increase the counterion density at the phosphate groups with a consequent effect on the orientation of the dye in the intercalation site. Also, the thermal unwinding of DNA at fixed ionic strength can be considered the result of the increased electrostatic free energy deriving from the reduction of the hydration and of the dielectric constant of the medium as well as from the increase of counterion dissociation. Thus, also at high temperature the ethidium orientation having the most extensive interactions with the DNA frame would be favoured.

Further information on the intercalation process can be gained from the variations observed in the neighbor exclusion range n. As pointed out in section 3, the value of n does not show any systematic dependence on salt concentration but increases substantially at high temperatures. Apparently, the local perturbation determined by the intercalated cation affects the structure of the duplex on a larger scale at high temperature than at low temperature. However, it has been shown [48] that high values of the parameter n can be found in case of site-specific binding when using theories based on a homogeneous lattice of sites in the analysis of the binding isotherms. It can thus be suggested that a binding specificity manifests, in the otherwise unspecific ethidium intercalation in DNA, at temperatures close to the duplex melting as a consequence of thermally excited conformational differences between specific base sequences. For instance, local fluctuations related to a base-pair opening process without unstacking, found to take place efficiently in double-stranded DNA [12,49], are considered by some authors [50] to play a determinant role in intercalation. This 'breathing' process shows only minor effects of salts but is noticeably dependent on the base sequence. It appears also to acquire cooperative character at temperatures close to the melting point. An increase in the average probability of the fluctuational base-pair opening from 10^{-6}–10^{-7} to about 10^{-3} has been calculated for heterogeneous DNA at respective temperatures of 50 and 10 degrees lower than the melting point [51]. At the same time, a range of variability of more than one order of magnitude has been predicted as a specific base sequences effect.

Taking into account that from molecular mechanical studies it has been inferred [52] that the energy required to form the intercalation site is a principal determinant in governing the base sequence preference for ethidium intercalation in DNA, we might consider the increase of n with temperature as evidence of the establishment of an increased preference for intercalation in (A + T)-rich sequences, where larger thermal effects on conformational fluctuations may be expected relative to (G + C)-rich sequences. This hypothesis appears to be consistent with the higher fluorescence quantum yield of the intercalated ethidium measured at high temperature if one attributes the binding preference for (A + T)-rich sequences to their ability to permit an increasingly better insertion of the dye when the temperature is increased. As a matter of fact, preliminary results on binding equilibria of ethidium to the duplex form of the alternating copolymer poly[d(A-T)] at room temperature [13] have shown fluorescence quantum yields of the intercalated ethidium about twice as high as those measured on CT-DNA along with values of the binding constants very similar to those found for CT-DNA under corresponding environmental conditions.

The results do not clearly define the relative affinity of the possible binding sites of the heterogeneous sequence of CT-DNA because of the interplay of structural and environmental effects on it. However, the variation of the quantum yield of the fluorescence of the bound dye strongly suggests that the intercalation of ethidium depends upon the sequence of the bases as a consequence of sequence-dependent conformation and/or mobility of the DNA duplex.

References

1 W. Saenger, Principles of nucleic acid structure (Springer, New York, 1984).
2 S.B. Zimmerman, in: Protein and nucleic acid structure and dynamics, ed. J. King (Benjamin-Cummings, Menlo Park, 1985) p. 279.
3 M.T. Record, Jr, S.R. Mazur, P. Melançon, J.-H. Roe, S.L.

Shaner and L. Hunger, in: Protein and nucleic acid structure and dynamics, ed. J. King (Benjamin-Cummings, Menlo Park, 1985) p. 313.
4 R.H. Sarma, Biomolecular stereodynamics (Academic Press, New York, 1981) vols 1, 2.
5 R. Rein, Molecular basis of cancer. Pt A: Macromolecular structure, carcinogens and oncogenes (A.R. Liss, New York, 1985).
6 C.-T. Zhang and G.-F. Zhou, Int. J. Biol. Macromol. 11 (1989) 165.
7 R.E. Depew and J.C. Wang, Proc. Natl. Acad. Sci. U.S.A. 72 (1975) 4275.
8 P. Anderson and W. Bauer, Biochemistry 17 (1978) 594.
9 A. Chan, R. Kilkuskie and S. Hanlon, Biochemistry 18 (1979) 84.
10 W.A. Baase and J.A. Shellman, Macromol. Symp. 1 (1986) 51.
11 G.S. Manning, Biopolymers 20 (1981) 2337.
12 E. Palecek, Prog. Nucleic Acid Res. Mol Biol. 18 (1976) 151.
13 E.F. Gale, E. Cundliffe, P.E. Reynolds, M.H. Richmond and M.J. Waring, The molecular basis of antibiotic action (Wiley, London, 1981).
14 J.B. LePecq and C. Paoletti, J. Mol. Biol. 27 (1967) 87.
15 R. Hudson, W.B. Uphold, J. Devinny and J. Vinograd, Proc. Natl. Acad. Sci. U.S.A. 62 (1969) 813.
16 R.T. Epstein and J. Lebowitz, Anal. Biochem. 72 (1976) 95.
17 T. Ide and R. Basuga, Biochemistry 15 (1976) 600.
18 J.C. Wang, J. Mol. Biol. 89 (1978) 783.
19 S.A. Winkle, L.S. Rosenberg and T.R. Krug, Nucleic Acids Res. 10 (1982) 8211.
20 J.C. Thomas, S.A. Allison, C.J. Apellof and J.M. Shurr, Biophys. Chem. 12 (1980) 177.
21 D.P. Millar, R.J. Robbins and A.H. Zewail, Proc. Natl. Acad. Sci. U.S.A. 77 (1980) 5583.
22 B.H. Robinson, L.S. Lerman, A.H. Frish, L.R. Dalton and C. Aver, J. Mol. Biol. 139 (1980) 19.
23 D.P. Millar, R.J. Robbins A.H. Zewail, J. Chem. Phys. 76 (1982) 2080.
24 D. Madge, M. Zappala, W.J. Know and T.M. Nordlund, J. Chem. Phys. 87 (1983) 3286.
25 J.C. Thomas and J.M. Shurr, Biochemistry 22 (1984) 6194.
26 T. Härd and D.R. Kearns, J. Phys. Chem. 90 (1986) 3437.
27 D. Genest and B. Malfoy, Biopolymers 25 (1986) 507.
28 M.J. Waring, J. Mol. Biol. 13 (1965) 269.
29 F.M. Pohl, T.M. Jovin, W. Baehr and J.J. Holbrook, Proc. Natl. Acad. Sci. U.S.A. 69 (1972) 3805.
30 C.-C. Tsai, S.C. Jain and H.M. Sobell, J. Mol. Biol. 114 (1977) 301.
31 S.C. Jain, C.-C. Tsai and H.M. Sobell, J. Mol. Biol. 114 (1977) 317.
32 A. Kindelis and S. Atkipis, Biopolymers 17 (1978) 1469.
33 M. Guenza, Ph.D. Thesis, Università di Genova (1989).
34 J. Greve, M.F. Maestre and A. Levin, Biopolymers 16 (1977) 1489.
35 T.M. Recard, Biopolymers 5 (1967) 975.
36 G. Guenza and C. Cuniberti, Spectrochim. Acta 44A (1988) 1359.
37 J.M. Ortega and W.C. Rheinboldt, Iterative solution of non-linear equations in several variables (Academic Press, New York, 1970).
38 L.M. Angerer, S. Gearghiou and E.M. Moundrianakis, Biochemistry 13 (1975) 1075.
39 W. Bauer and J. Vinograd, J. Mol. Biol. 47 (1970) 419.
40 J.L. Breasloff and D.M. Crothers, Biochemistry 20 (1981) 3547.
41 W.D. Wilson, C.R. Kirshnamoorthy, Y.-H. Wang and J.C. Smith, Biopolymers 24 (1985) 1941.
42 E.C.W. Clarke and D.N. Glew, Trans. Faraday Soc. 62 (1966) 539.
43 J.W. Nelson and I. Tinoco, Jr, Biopolymers 23 (1984) 213.
44 D.M. Crothers, Biopolymers 10 (1971) 2147.
45 H.J. Li, Biopolymers 12 (1973) 287.
46 D. Stigter, Biopolymers 16 (1977) 1435.
47 B. Norden and F. Tjerneld, Biopolymers 21 (1982) 1713.
48 R.H. Shafer and M.J. Waring, Biopolymers 21 (1982) 2279.
49 J.D. McGhee and P.H. von Hippel, Biochemistry 16 (1977) 3267, 3276.
50 H.M. Sobell, in: Nucleic acid geometry and dynamics, ed. R.H. Sarma (Pergamon Press, New York, 1980) p. 289.
51 R. Wartell and A.S. Benight, Biopolymers 21 (1982) 2069.
52 T. Lybrand and P. Kollman, Biopolymers 24 (1985) 1863.